

Non-Equilibrium Flow Type Behaviour In Presence Of Transonic Free Streams Probably Caused By Turbulence Modeling Limitations For Base Flow Computations Using N-S Code, As Well As BASE2D Codes.

A.P. Roychowdhury
Aerodynamics R&D Division , Vikram Sarabhai Space Centre, Trivandrum,
Pin 695022,Kerala, India.
ajoyroy_chowdhury@vssc.gov.in

Abstract

The computational difficulties in getting the flow field using a RANS solver of base flows is given here in two special cases where results were obtainable only when free stream flow was not considered. The computational difficulties could be attributed to frequency shift in both theoretical as well as experimental results caused by small vibrations and large discretizations across the path-line of the base flow.

Keywords

Lower temperature thermodynamic non-equilibrium; N-S analysis; semi analytical inviscid - viscous interaction; closed flow analysis; neglecting free stream; frequency shifted analysis

1. Introduction

This preliminary analysis of lower temperature thermodynamic non-equilibrium study in base flows consists of studying two types of problems. One is based on solution of the Navier-Stokes equations for analysis of the base flow and another one is based on the analytical model for studying the base flows with a closed flow modeling for obtaining computational solutions. In the N-S analysis, CFD software was used to study the flow field using Navier Stokes solver for the for two gas problem which involves the interaction only between multijets of central motor and strap-ons. Here free stream flow was not considered. We found that the flow field in the multijet interaction region where shock cells were resolved and found initiation of reverse flow at that flow condition. In the analytical analysis we studied the problem using BASE2D code where a special problem of a typical launch vehicle without strap-ons and interacting flow field analysis of central jet with the free stream was considered with free stream modeled as a jet. It was seen from the results that base pressures and base heat fluxes could not be computed using BASE2D code. The computational difficulties could be attributed to frequency shift in both theoretical as well as experimental results caused by large discretisations across the path-line of the base flow.

One of the major thermodynamic problems encountered by launch vehicles during their power-phase operation is the problem of base heating. This arises due to the (momentum and thermal) energy transfer from the engine exhaust gases to the base region. This problem has been identified for some time as a significant factor of concern in regard to the structural integrity of the vehicle base area. Several years ago, the early flights of Atlas, Jupiter and Titan launch vehicles failed due to excessive heating of the base region from the exhausts of the first stage engines, which had a reverse flow in the base region due to the interaction of the plumes of core engine with strap-on jets and even jet-free stream interaction. As suggested in the title in transonic free stream flow generally encountered in base flow problematic regions, the K-Epsilon turbulence model fails which otherwise works in continuum aerodynamic flow situations. It fails to converge in such flow situations and we have given reasons for such a failure but nothing is yet clear and it will push other researchers to look into pointed issues as given in conclusions *viz* frequency shifted nullity condition, feedback disturbance phenomenon and also lower thermodynamic non-equilibrium issues. Two alternate methods for solving such problems are also given at the end. Flight results experimental data are mentioned though exact numbers are not given as it is beyond the scope of this work.

Any overall design of a launch vehicle requires a complete analysis of the base flow for each configuration and flight environment. Further base heating occurs at high altitudes in a manner different from that at low altitude for the same vehicle.

The first really convincing and physically realistic base flow models were proposed in the early 50's by Chapman (1951) and Korst (1956). Mostly all practical methods for base flow calculation are based on the work of Korst. In the literature, these classes of methods are named as multicomponent method. Practically at the same time, Crocco and Lees (1952) proposed a different approach which allows, in principle, gives a more satisfactory representation of a flow containing the important viscous region. This approach is called the inviscid-viscous interactive method. Although widely used in many complex aerodynamic flow computation, its use in predicting the base flows is limited due to inherent complexities of the method. This method presently has become outdated because N-S solvers have now the capacity to solve for both viscous and in-viscid regions in a short time, especially by employing parallel computation techniques.

The basic idea of inviscid-viscous interactive methods and multicomponent methods consists in splitting the flowfield into

- An external or outer region where the viscous terms are assumed to play a negligible role.
- One or more several inner regions in which viscous effects are essential. These regions are boundary layers, mixing layer, jet, wake etc.

Two different ways are proposed to formulate the inviscid-viscous interaction problem

- 1 The first one consists in dividing the flow field into distinct regions which are separated by a boundary and described by different equations. The two sets of equations are solved independently; their solutions have to satisfy compatibility coupling conditions along the boundary.
- 2 In the second technique, one considers a continuation of the external inviscid flow into the region normally occupied by the viscous flow. The compatibility conditions are written on a surface embedded in viscous part. Most often the surface is the displacement body i.e, the body surface augmented by the dissipative layer displacement thickness or the wall itself. This method is used in BASE2D code developed at VSSC which we have used to get some results of jet-free stream interaction.

In the multicomponent methods which apply essentially to base flows containing large separated region, the dissipative layers are represented by simplified analyses incorporating a relatively large dose of empiricism. The compatibility of these regions with the fully in-viscid flow is expressed in a rather coarse manner by satisfying continuity of pressure (no shocks in the reverse flow region) and velocity (no vortices in the reverse flow region). Two important conditions have to be defined for this simplified base flow analysis.

1. determination of the mixing properties at the point where the re-attachment phenomena begins
2. Determination of the condition to express the uniqueness of the solutions; namely the "re-attachment criteria".

For most practical applications, multi component method remains the essential predictive tool due to their general acceptable level of accuracy in the prediction of the most important flow feature and their low computational cost. These methods are capable of predicting base flow including effects of centered propulsive jets, base bleed, heat flux, mixing of different species and turbulence modeling.

Although the scope of this present survey is to review the semi-empirical & analytical approaches which are used to determine the base flow, a brief review of the CFD techniques in the base flow computation is also presented. A CFD software that simulates flow over arbitrary complex bodies by solving compressible 3-D Navier-Stokes equations has been used in the present study of base flows. It uses an adaptive Cartesian grid system that adapts to geometry as well as to the flow gradients as the flow evolves through a series of time steps. The software has very user friendly with pre and post processors that help in setting up the problem defining the computational domain, boundary conditions, free stream conditions, and importing geometry through IGES format and setting up the convergence criteria. All these features are handled by the pre-processor. Post-processor helps in viewing flow parameters obtained from the flow field solution, extracting field values of parameters and also getting overall forces & the moments on the bodies. The software can handle structured body oriented grids, internal flows, two phase flows as well as non-equilibrium chemistry using up to a 7-species 25 reaction model. The CFD software incorporates a standard k- ϵ turbulence model.

It should be said that in spite of the spectacular progress made in base flow computation, the semi-empirical formulae are still extremely precious in making the estimation of the base flow, particularly in situations where detailed theory is still lacking or still un-reliable.

Discussion on base heating includes two basic mechanisms by which energy is transferred from the engine exhaust gases to the base region of the vehicle.

- Convective heating
- Radiative heating

Convective heating is caused by hot rocket exhaust gases which recirculate towards the base. This recirculation can occur due to the interaction of the exhaust jet, either with the external body flow, or with another exhaust in the case of multi-nozzle rockets under certain operating conditions. The external air stream separates from the body at the base corner and converges toward the nozzle axis of symmetry. This creates a base region which is separated from both the external free stream flow by free shear layers. The inner parts of these shear layers have low momentum and flow in these parts cannot negotiate the pressure rise that results from recompression both up-stream of the stagnation point and downstream. Some of the hot rocket exhaust gases turn back towards the vehicle and are at high speeds and heat the base. The problem is considerably more serious in multi-nozzle rockets due to the possibilities of additional jet interactions. In this rocket there will be extreme lateral expansion of the jet plumes at high altitudes, because the jets become highly under expanded.

Base heating can result from radiation from the jet after-burning plume. Heating in the base region from cluster engine is caused mainly by radiation at low altitudes; however at some intermediate altitude (7.5 km to 15 km) reverse flow begins to occur, and convective heating becomes the predominant mode of heating.

Radiative heat transfer from the plume to base is fairly obvious. Regions of high temperature can exist in the jet. In some cases, at low altitudes there can be secondary combustion of fuel-rich engine exhaust with air, and radiation could be dominated by this factor. In the case of multi-rocket vehicles, there will be significant interaction between the exhaust plumes because of their extreme lateral expansion at high altitudes where the ambient pressure is very low. In some cases the interaction may be severe enough to produce very high temperature reverse flow regions as a result of the formation of oblique intersecting shocks. Radiative heating problems may also arise due to the presence of these high temperature regions. These radiative fluxes are evaluated independently of convective fluxes caused due to reverse flow.

Some launch vehicles contain a core engine with two or more thrust motors strapped on to the engine-case, for thrust augmentation. Based on mission thrust requirement patterns, the strap-on motors can be designed to be in simultaneous powered-phase operation with the central engine, or the central engine may be idle while the strap-on motors are firing. In the former case there is a distinct possibility (which can be determined by jet plume calculations for flight conditions in the designed mission) of interaction between the central engine exhaust and strap-on engine exhausts. In case there are more than two strap-on engines, there can be interaction between the various strap-on exhausts themselves. Both the above types of interaction can create base heating problems due to reverse flow upstream of interacting shocks.

When there is no interaction of the two exhaust jets, base heating is not expected to be any more serious than in a single-engine rocket interacting with free stream-jet. But if they do interact there is reverse flow of hot exhaust gases and significant base heating might result. Here as discussed later, because of limitation of turbulence $k-\epsilon$ model of CFD software, viz. PARAS code, as well as thermal non-equilibrium effects, we were able to study the less serious interaction namely only the jet-jet interaction without effects of free stream being accounted.

This analysis using BASE2D code to evaluate the mass, momentum and energy of gases turned back toward the base from the interaction of central exhaust jets with free-stream. First in-viscid jet boundary and then flow properties are determined using the semi-analytical BASE2D program developed at Aerodynamics Research and Development Division of VSSC. Oblique Shock compression of the two jets is considered to occur at the intersection of these boundaries such that the pressure rises to a common value. If the two jets are identical, flow direction downstream of the compression is along the centerline of the two interacting jets. Mass and energy balance between the jet boundary stream line and the discriminating streamline (displacement streamline or reattaching streamline) gives the reverse flow mass flow rate and thermal energy. BASE2D code is a lumped analysis of mass, momentum and energy which represents a zero dimensional model, which however can replicate coarsely the three dimensional flow in the base.

3 Analyses

The description which follow is done in 3 sections

- (A) The description of the code and the problem solved using RANS CFD code PARAS,
- (B) The description of the code and the problem solved using semi-analytical code BASE2D with an implicit RANS formulation for the mean velocity profile and
- (C) Paradoxical behaviour exhibited by various codes referred to or used by the author with co-workers, different from the present work. These remain unpublished which are related to frequency shifted phenomena associated with limitations and sometimes having advantages.

2.1 Section (A)

The base flow analysis is made for the first stage of a launch vehicle. For the launch vehicle considered the first stage consists of only the main engine, and there are six firing strap-ons. The interaction between the strap-on and the core jet from the main engine is considered without considering free-stream jet interaction. Using PARAS-3D the flow field analysis is carried out to find whether this interaction induces a reverse flow. The base pressure and base convective heat flux are calculated using theoretical analysis from data obtained from PARAS N-S solver. Heat transfer at the base region is by stagnation point heat transfer formula of Fay and Riddle (1958). The formula is derived after making some approximations on the numerical solution of chemically reacting boundary layer flow at stagnation point, under equilibrium conditions.

Thermal non equilibrium

When the temperature field varies very irregularly from point to point in space, such flows represent thermal and chemical non-equilibrium flows. This generally happens at very high temperatures where the gas flow is in a disassociated and ionized form. Here the definition of enthalpy $H = CpT$ does not hold. Vibration modes of the atomic spectra are predominant than rotational and translational modes. However we find it existing in base flows as well, as will be discussed later, but which is generally associated with lower temperature phenomena. The transonic flow singularities manifest as pressure and entropy waves which coalesce and form shock waves which are oscillating and cause the effect of problematic equation of state and cause lower temperature thermodynamical non-equilibrium

PARAS 3D, an acronym for PARAllel Aerodynamic Simulator, is an in-house developed software. This is a numerical flow simulation software (CFD) that can simulate viscous, turbulent, three dimensional fluid flow over arbitrary three dimensional bodies. It operates on a parallel computer system consisting of a cluster of workstations or Pentium PCs. The code can solve viscous or inviscid flow using finite volume method on a Cartesian grid. The time stepping is done for each cell based on local CFL criterion and fluxes at the interface of the cell are computed by means of an approximate Riemann solver. The explicit scheme is second order accurate in space and of TVD type which is achieved by means of a limiter of the min-mod type. As the solution proceeds, the flow can be refined by adding more grids at regions of high flow gradients and at the same time removing extra cells around regions of low flow gradients. The code has a pre and post processor based on graphics library GLIB. The code is very user-friendly and can be easily customized based on our requirements. Automatic grid generation capability is also present which essentially consists of a capture level and a refinement level by dividing the parent Cartesian cell into 8 cells. Irrespective of the complexity of the geometry, grids can be automatically generated from the cross-sectional details which can be obtained from any 3D geometry modeling package like AutoCAD, CATIA etc. for relatively simpler geometries, either the user can write his own program using 'C' or use the pre-processor of PARAS 3D to generate the initial grid.

It can solve either Navier-stokes or Euler equations. It has an in-built K-Epsilon turbulence model. The wall effects of the turbulent flow are modeled by a modified wall function approach.

The grids get adapted automatically based on body geometry during grid generation and based on the flow gradients, during solution procedure.

The grid around the body is generated by means of a Rectangular Adaptive Cartesian Mesh technique. Cartesian cells used in the code are basically of 3 types. These are,

Cells which are fully outside the body (air cells)

Cells which are fully inside the body (body cells)

Cells which are partially inside the body and partially outside the body (partial cells).

Using a coarse mesh initially, and later a capture level and refinement level and Rectangular adaptive Cartesian mesh method the grid is generated.

The solution strategy in PARAS 3D, is to march in time, in a local time stepping mode for faster convergence. The interface fluxes are calculated by means of an approximate Riemann solver and the explicit solution scheme is of Total Variation Diminishing (TVD) type. In PARAS 3D, the following 4 options are available in the solver module,

1. Euler solver
2. N.S. Turbulent solver
3. N.S. Laminar solver
4. 3 gases solver (mixing of 3 different gases. viz : core jet, strap- ons jets and in the presence surrounding air during lift-off)

In case of Euler and laminar N-S solver, the coupled flow equations are solved for ρ , ρ_u , ρ_v , ρ_w , ρ_z , $\rho C_v T$ where z is the mass fraction. In case of turbulent solver, additional equations for variables pk and pe that is kinetic energy and dissipation of turbulence are also solved. In the case of 3 gases solver, an additional mass fraction

equation for the variable (ρ_{z1}) will also be solved. The turbulent solver uses the K-Epsilon model to model turbulence. The wall damping effects of the turbulent flow are considered by means of modified wall function approach without resolving main structure and exact velocity profiles in the boundary layer.

In this code, the different types of field boundary conditions are available which can be implemented at the boundary of the computational domain, these are,

1. UPWIND: In this case, the free stream values of the flow variables are imposed at the boundary of the domain.
2. SHIFT: In this case, it is assumed that flow gradient is zero at the boundary. It is same as supersonic out flow condition.
3. SYMMETRY: In this case, symmetry condition is applied at the boundary. All the flow variables have zero gradients across the boundary except the velocity normal to the boundary which is non zero.
4. PRESSURE: In this case, the outflow is subsonic condition.

These conditions need to be specified on all the six faces of the computational domain while describing the configuration file of the problem. Generally we use the condition Neumann for Euler flows and modified wall function or Dirichlet for other flows. At the wall the above specified boundary conditions can be applied.

The geometry used for the analysis is that of a typical launch vehicle having central motor and strap-on motors. The geometry was generated in PARAS code and the jet flow exhaust properties are given in Tables 1 and 2 respectively for a particular time instant time after launch. This instant is where the pressure at base switches from being below ambient to that of being above ambient. First the problem was solved as a 3-gas problem where the k- ϵ turbulence model in PARAS code is invoked. The pressure ratio for the case is around 0.88 for the core jet. To initiate calculation we start with a jet pressure ratio of 0.83 and gradually increase it to 0.88. However, we did not carry out any analysis to find the cause of the blow-up and this aspect also needs to be looked into.

As discussed later this above 3-Gas problem blows up after 1000-2500 iterations. Hence the problem was simplified to a Euler solution problem with only 2-Gas problem *viz* the central motor and strap-on interaction study.

2.2 Section (B)

The evolution of analytical methods for predicting the effect of plume interactions on the base has not kept pace with the development of testing techniques and acquisition of data. The complete base flow model is composed of multi-component analyses which are classified in to three categories:

1. Inviscid plume effects,
2. Inviscid (expansion shockwave, recompression shocks in both upstream and downstream regions of stagnation point which is at the intersection of two oblique shocks as predicted by Latvala 1959 code) as well as viscous flow modelling in the jet interaction regime which results in reverse jet and
3. Impingement of the reverse flow from jet on the vehicle base.

This analysis can serve as a basis for base heating predictions.

In BASE2D analysis we have a mass balance, momentum balance and energy balance equation. However, this analysis represents interaction of two jet plumes at a time and multi-jet interaction model is necessary to be formulated.

Mass balance equation:

Mass flow rate near the base can be written as

$$\int_1 \rho u dy + \int_2 \rho u dy = 0$$

Energy Balance Equation:

The conservation of energy in the base region requires the total energy flux to be zero. The equation of energy flux near the base can be written as

$$T_b/T_{01} = (T_{0r}F+G)/(F+G-(1-\tau)H)$$

$$F = T/Wm (2 \int (\rho/\rho_2) \Phi^2 d\eta) - ((\rho/\rho_2) (d \Phi/ d \eta))$$

$$G = (2 \int (\rho/\rho_2) \Phi^2 d\eta) - ((\rho/\rho_2) (d \Phi/ d \eta))$$

$$H = 2 \int (\rho/\rho_2) \Phi^2 d\eta$$

The convective heat flux & the base pressure be predicted by the above formulation using the Crocco's energy & Buseman's integral relations given as,

$$\rho/\rho_2 = T_2/T = (1-C_2^2)/((T_b/T_{01}) - (C_2^2 \Phi^2))$$

Where C_2 is the Crocco's number defined as

$$C_2^2 = ((\gamma-1)/2 M_2^2) / (1 + (\gamma-1)/2 M_2^2)$$

Subscript '2' indicates the reverse flow in base region; Φ is the turbulent velocity profile defining function⁶ in base regions and subscript '1' represents ambient conditions and integration limits are across the shear layer of the two jets. α is the mass fraction ratio.

Procedure for BASE2D analysis:

1. A trial value of P_b/P_α and T_b/T_α is selected
2. Next the in viscid flow field and boundary for both the external flow and the central jet is computed and the point of flow reversal obtained.
3. The jet boundary streamline Φ_j is computed from the mixing layer analysis by iterative means.
4. The discriminating streamline is then computed by re-compression pressure rise analysis.
5. The entrained mass flow can be computed for the external and the central jet flow respectively.
6. Finally energy transfer analysis is made.
7. An iteration scheme modifies the guessed values of P_b/P_α and T_b/T_α until the mass balance and energy balance equations are satisfied and a unique base flow solution is obtained. ' α ' represents free stream conditions.

The turbulent velocity profile used is the error function implying mean velocity profile.

This problem was solved by the BASE2D code assuming the free stream as a jet and interaction with core motor alone.

2.3 Section (C)

With reference to this above mentioned work and the method of solution used in this work we discuss the following:

(1)

First of all we would like to mention of a modified equation of state used in a Lattice Boltzman's equation solver indicating the need to consider low temperature thermodynamic non-equilibrium (Yuan and Schaefer (2006)). Also, finite volume techniques (F.V.) have always to be solved with a phenomenological turbulence equation because conservative estimates have been made to flow parameters where extra and unnecessary terms may appear which need to be filtered out by turbulence models.

Same thing happens in solution procedure discussed in above paper (Visbal and Gaitonde (2002)) where conservative estimates have been made by Thomas and Lombart (1979) for grid differencing with respect to moving grids where metric errors are reduced. However the solution is proceeded with finite difference technique (F.D.) for conservative fluid dynamical N-S equations by beam and Warming implicit technique together with metric corrections and spatial differencing implying doing a filtering.

(2)

The ailing errors for finite difference schemes can be overcome by using higher order compact schemes together with suitable stencils for wall conditions. For finite volume schemes we can use either flux vector or flux difference schemes. From other findings of CFD analysis we see that flux difference schemes Roe's solver with artificial dissipation terms gives solutions in close agreement with flux vector schemes, like van Leer's and TVD schemes. However it is also seen that the algebraic Baldwin Lomax and Spalart Allmaras model works well with high Reynolds numbers case like the $k-\epsilon$ turbulence model. Also close comparisons of wall quantities of heat fluxes represented by Stanton number and pressure represented by coefficient of friction match well with experimental results only when small wall vibrations are present. Alternatively explicit solver can be accelerated to convergence by multi-grid solvers where spatial averaging across cell faces is made.

(3)

Also in PARAS solutions for $k-\epsilon$ turbulence model for quick convergence with respect to convergence factor is obtainable only when the CFL number is reduced after every 100000 iterations is reduced drastically to make the scheme stable. For first 1000 iterations CFL number of 0.2 is chosen and reduced to 0.05 upto 10000 iterations and when successively reduced and refined the convergence is obtainable within 40000 iterations. This is for even highly under-expanded jets. Also the NS equations is a second order partial differential equations which together with boundary condition is seen to give infinite number of solutions. But in a turbulent flow after period three bifurcation it goes to chaos with a fractal dimension of three plus. But a chaotic system is very sensitive dependent on initial guesses as found from strange attractor theory. Hence in computations different initial guesses will give different steady state solutions. Then how can grid refinement together with CFL number reduction reduce it to a converged system which gives a unique solution for different

initial guesses. This can be credited to a benevolent factor of frequency shifted effects. Further in such cases the cold stream $k-\epsilon$ turbulence model need not suffice and modern day one of the implicit turbulence models in large eddy simulations need to be considered in NS solvers so as to give solution for same order of CFL number chosen. Alternatively, one can also invoke multi variate analysis by invoking matrix perturbation techniques and then doing a least square fit to the obtained data sets and following it by regression analysis.

(4)

Another finding which we wish to emphasize is that on Euler's solution on 2D unstructured grids obtained by Denauley triangulation we get converged results, but when viscous terms together with $k-\epsilon$ model is incorporated we find that the system diverges even for low Reynolds numbers. We found a similar behavior when we obtained neutral curves for non-isentropic compressible flows which showed stable regions when Reynolds number was as low as 250 for Mach number flows between 0 and 2.0 (Roy Chowdhury (1994)). However experimental results from literature show a different value.

(5)

Also the author wishes to report the work of his work with co-workers on obtaining the turbulence characteristics of data obtained of the atmospheric boundary layer carried out using MONTBLEX (monsoon through boundary layer experiment) data. The Kolmogorov's $-5/3$ power law was found to be un-reproducible and a 50 % dispersion band was observed showing once again dispersion due to the frequency shifted effects.

(6)

Also we may add that sound radiation are due to entropy fluctuations interacting with polar sources sent as electromagnetic waves at a wavelength so that when it interacts with ambient it reconverts as pressure waves of sound. The source term linearization required in computation radiative heat transfer analysis and also found in basic solution strategy for jet stability analysis, is actually introducing orthonormalization in the interior layers and ergodicity exists at the boundaries especially for highly under-expanded jets having a simple flow field. However this condition exist in cases of single jets only and not for multi-jets at large under-expansion ratio, where non-ergodicity and lower temperature thermodynamic non-equilibrium dominate.

3 Results and discussions

In base flow analysis using PARAS-3D the interaction of jets of central engine and strap-ons together with free stream flow was attempted. We choose a test case corresponding to exit conditions of central jet, strap-on jet and free stream at a particular instant from lift off, where base pressure and base heat flux do not indicate the same phenomena. To study this anomaly this work was undertaken.

We first attempted an open flow study described as follows. The procedure involved defining the body of a typical launch vehicle. Next the grids have to be generated around the body. The dimension of the flow field was -20m from the origin to 120m from the origin and 40m in the cross-stream direction. The origin is at the centerline of nose cap of the vehicle. Earlier a -10m/100m/20m flow field domain was tried out but we did not get the converged results. Hence the larger domain was chosen which was -20m/120m. This was done for allowing of upwind with the help of the solver. As described earlier, the steps in grid generation was invoked and the grid was automatically generated. Allowing for clustering in the base region for grids, the grids were generated. The following data gives the overall results of the grid generation

Total number of grid cells = 1739964

Gas cells = 1123424

Part cells = 398180

Body cells = 218360

After the grids were obtained for standard $k-\epsilon$ parameters the 3gas problem was attempted using 3-gas solver of PARAS. The inputted jet parameter for core, strap-ons and free stream are given below and also given in tables 1, 2, and 3.

Jet 1 parameter – core

Mach number = 3.254000

Pressure = 53940.000000

Density = 0.059480

Gamma = 1.200000

Molecular mass = 0.025000

Jet 2 parameter – strap-on

Mach number = 3.016100

Pressure = 55000.000000

Density = 0.058000

Gamma = 1.200000

Molecular mass = 0.025000
Free stream parameter
 Alpha (α) = 0.000000
 Beta (β) = 0.000000
 Density (ρ) = 0.824900
 Pressure (p) = 66148.500000
 Mach number = 0.905000
 Molecular mass = 0.028800

TABLE 1
 CORE NOZZLE AND EXHAUST PROPERTIES

1	Nozzle chamber gas temperature(K)	3323.0
2	Exit gas molecular weight	25.0
3	Exit gas specific heat ratio	1.20
4	Area ratio of nozzle	9.1
5	1/2 cone angle of nozzle (deg)	15.420
6	Exit Mach number	3.2540

TABLE 2
 STRAP-ON NOZZLE AND EXHAUST PROPERTIES

1	Nozzle chamber gas temperature(K)	3323.0
2	Exit gas molecular weight	25.0
3	Exit gas specific heat ratio	1.20
4	Area ratio of nozzle	6.58
5	1/2 cone angle of nozzle (deg)	15.83
6	Exit Mach number	3.0161

TABLE 3
FREE STREAM PROPERTIES FOR CFD SIMULATIONS

1	Molecular Weight	28.0
2	Specific heat ratio	1.4
3	½ cone angle (deg)	1°
4	Exit Mach number	0.9050

Area ratio Mach number equation was used for obtaining from the exit diameter (which is 10 times core motor exit diameter) the throat diameter of free stream. This data given above is used both for N-S analysis as well as BASE2D analysis. Also Table 4 gives the input and output of BASE2D code for a special test case.

The Courant number of the problem was taken as 0.4. We run the solver for case when the strap-on exit pressure was changed to 52500.0 and the free stream pressure was changed to 60000.0 for starting computations with a lower jet pressure ratio. This was done to allow for a smaller jet pressure ratio for starting computations. However it was found that when this problem was solved more than 5000 iterations, the solution blow up. Hence we choose the solution for 1000 iterations for this initial guess for the actual problem where the strap-on pressure was 55000.0 and free stream pressure was 66148.5. This solution was run using initial flow field at 1000 iterations of the previous case. However at 2235 iterations the solution blows up. This was seen because the convergence factor (CF) jumped from 9.079 at 2234 iterations to 330.7 at 2235 iterations.

This failure in this first attempt in an open flow study could be accounted to two reasons viz, namely turbulence model did not work properly and lower temperature thermodynamic non-equilibrium effects in the flow field which could have been driven due to the faulty turbulence model or the flow field itself. This is because a perfect gas equation was used in the solver which holds for lower temperature gas and this led to problems. The experimental results showed that the actual flow field was not of high temperature so as to cause non-equilibrium of flow, so low temperature thermodynamic non-equilibrium was a strong candidate for such behaviour. Another probability could be artificial dissipation effects which accumulated and diverges the solution. Similar problems were also seen for our previous study using -10m/100m case for various flight conditions and reasons for such problems are same as discussed above. Here it should be noted that the Courant number was reduced to 0.2 which generally considered as the lower limits for PARAS solution. Since no low temperature thermodynamic non-equilibrium models exist in literature we could not go on further with such open flow analysis. The number of cells was approximately 17 million which is a reasonable amount of cells for such a problem.

So we decided to see what happens and analyze the flow using a closed flow analysis by not considering the free stream and solved the problem using the Euler 2-gas solution of PARAS of two interacting jets. Here we started with same case of lower pressure of 52500.0 for strap-ons and went till 1000 iterations for a Courant number of 0.4. Then we changed the Courant number to 0.2 and increased the strap-on pressure value to 55000.0 which is the specific case situation we are trying to solve for the same grid as that of 3-gas problem attempted earlier. We ran the problem till 30,000 iterations; we found that the solution was converged by then. Such a large number of iterations with a CF number of less than 1 is considered as a converged solution. The results of the converged solutions are given in figures 1 to 4.

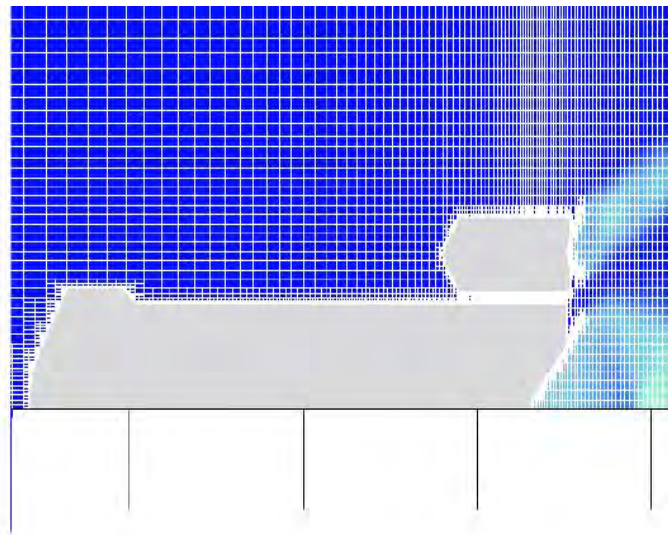


Figure.1 Blown-up view of grid distribution .

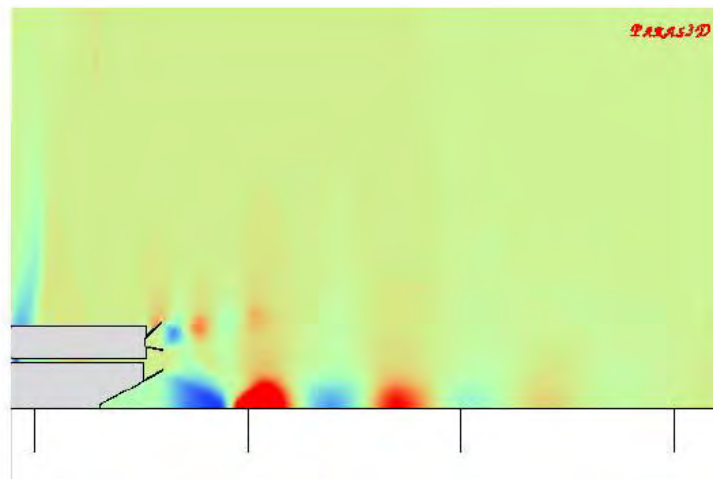


Fig.2 Blown up view of pressure palette.

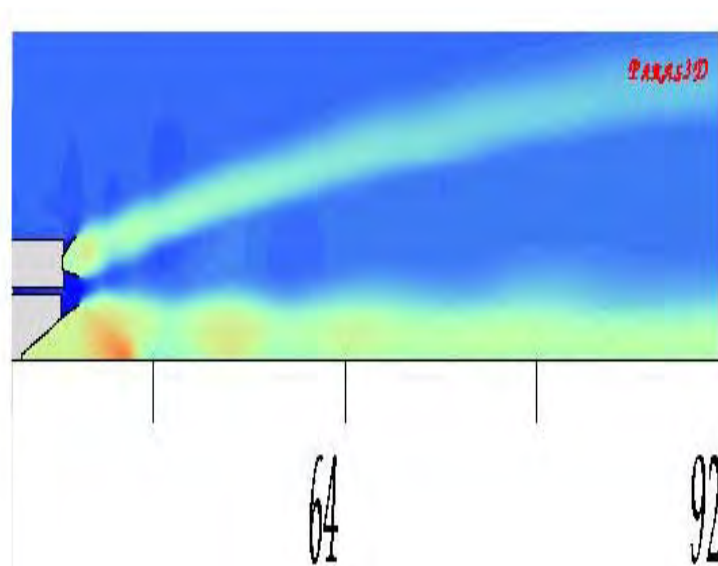


Fig.3 Blown up view of Mach number palette.

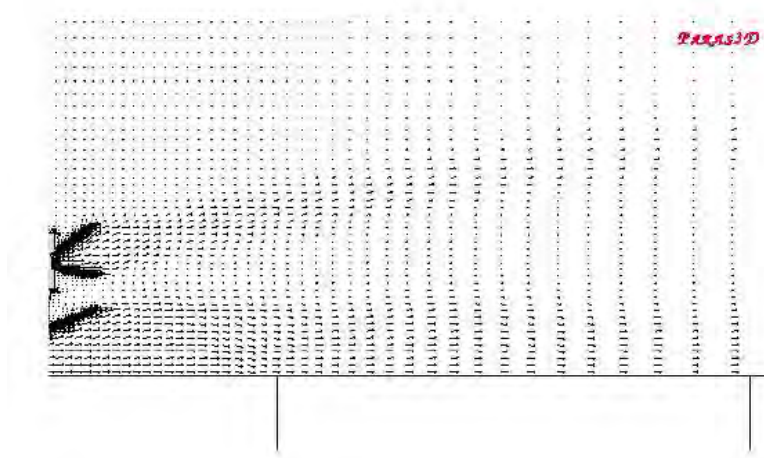


Fig.4 Blown up view of u,v,w vector plot.

For the closed flow system , Figure 1 shows the blown up version of the grid. Figure 2 shows the pressure plot of the body blown up view. Figure 3 shows the Mach number plot of the body blown-up palette. Figure 4 shows the uvw vector plot in the blown up view. Here the ambient pressure was the pressure at the particular altitude and density properties corresponded to that altitude. Only the free stream effects were absent. The results obtained showed shock discs of both the jets and the interaction regime as seen from Figs. 2, and 3. It was seen that there was a slight amount of reverse flow in this interaction regime, when it was resolved using the uvw vector plot (Figure 4). This effect was also indicated in our flight results but as seen from PARAS simulation the reverse flow velocity was very small. Hence the heat flux effects were absent. Reverse flow could also be induced because of artificial dissipation effects during the solution of this problem.

In our second problem, we solved the an closed gas flow problem of a typical launch vehicle with core alone and free stream modeled as a jet and no extra –fictitious free stream is considered. This feature does not generally get accounted in BASE2D code, because the standard problems involved only multijet interaction without free stream effects. The problem was checked with the free stream being modeled as a jet having a thickness of double the case presented and there was no change in the results. This analysis was carried out for a special case of maximum base-heat flux motor condition. Here also we find, that the base pressure which should higher than the ambient pressures as found in flight data does not happen in computational results and pressure and heat-flux results are given in Table 4 where choking occurs in upstream in free stream and results of convective heat flux of 1.5 W/cm² are not obtainable. Another feature of base flows is that at higher altitudes the reverse flow which generally has a 3-D relief shows choking of the relief flow thereby causing a rise in base pressures. Also, at higher altitudes when plumes interact the intersecting shock is stronger and the reverse flow has more energy. This phenomena generally gets terminated because of fall in the chamber pressures of the motor of the jet during its trail off-conditions.

TABLE4
BASE FLOW RESULTS OF FREE-STREAM-JET INTERACTION
INPUT DATA FOR BASE2D CODE

Telemetry time (s)	Altitude (Km)	Mach no.	Chamber press of core (Mpa)	Chamber press of s/o (Mpa)
85.0	27.807	2.868	4.046	0.0565

TABLE FOR GENERATING INPUT TO BASE2D CODE

Altitude (km)	Mach no	Diameter of throat (m)	Distance of throat to exit (m)
27.059	2.868	6.1582	164.47

(BASE2D RESULTS): FREE- STREAM MODELLED AS JET

Telemetry time (sec)	Altitude (km)	Atm. Pr (Pa)	Base Pr (Pa)	Total Temp (K)	Static Temp (K)	H.F.rate (W/cm** 2)	Mach No. of Free stream
85.0	27.059	1878.94					2.868

One may say that the cause of lower temperature thermodynamic non-equilibrium could be accounted to the system being analyzed as an open system in the free stream thickness considerations. If the free-stream is considered of small thickness then the system is of closed flow type and the feedback mechanism of instability caused disturbances from shock cells to the nozzle lip occurs and this converges the numerical solution of N-S solvers and it does also plays an effective role in BASE2D flow computations. Frequency shift effects (Roychowdhury (2003)) due to vibrations of the nozzle with respect to the path-line of flow for cold streams in transonic, supersonic and hypersonic regimes could be also the cause of solutions in BASE2D problem to give results which are not consistent with experimental data. The NS solutions obtained requiring closed flow analysis can also be accounted for frequency shift problems across pathlines.

From the closed flow, NS analysis, PARAS-3D software was used to study the flow field using Euler solver analysis for two gas problem which involves the interaction between multi-jets of central and strap-ons for a particular instant of time for a typical launch vehicle system. Here free stream flow is not considered. We find the flow fields in the multi-jet interaction region where shock cells were resolved and shock cells were seen and reverse flow effects were also seen. The N-S analysis for the open flow analysis for the 3 Gas problem failed either due to thermodynamic non-equilibrium effects, and/or faulty turbulence modeling and/or artificial dissipation induced numerical noise.

From the closed flow multi-component type semi-analytical analysis we studied the problem with BASE2D code where a special of a typical launch vehicle without strap-ons and flow field analysis of central jet with free stream was considered. It was seen from the results that base pressure and heat flux are far off from flight data.

Based on earlier analysis of different problems of shear flows studied from a linear (Roychowdhury and Sreedhar (1997), Roychowdhury and Sreedhar (2000) and Roychowdhury et al (2000)), weakly non-linear (Roychowdhury (2005)) and fully non-linear stability point of view, introducing concepts such as isentropic (Roychowdhury et. al. (2000)), non-isentropic (Roychowdhury and Sreedhar (1997), Roychowdhury and Sreedhar (2000) and Roychowdhury (2005)), finite and infinite rate chemistry and equilibrium turbulence models have been made for studying routes to turbulence. This route can be classified with initial disturbance, linear stability, weakly non-linear stability, non-linear stability, initial turbulence, fully turbulent and decay of turbulence, and one finds the system is full of anomalies sometimes representing a 2-dimensional system as a 3-dimensional system (Roychowdhury and Sreedhar (1997), Roychowdhury and Sreedhar (2000) and Roychowdhury (2005)) and vice versa (Roychowdhury et al (2003)). Further, isentropic analysis (Roychowdhury et al (2000)) was able to show the quick and short length self-similarity behaviour of highly under-expanded jets (having large jet to ambient pressure ratios). Further in analysis of Gaster's transform (Roychowdhury and Sreedhar (1992) and Gaster (1962)), which relates the spatial growth rates to temporal growth rates using Group velocity as the connecting parameter, it was shown that it is valid only for the zero growth rate case and hence represents neutral disturbance cases only. One wonders what is the cause of such behaviour in transition and turbulent flows. It can be considered that the feedback mechanism analysis between the interacting shocks and lip of nozzle causes both the closed flow analysis done by us to give results matching with experimental data. For jet flows or multi jet flows which have high or moderately high convective Mach number, the zero thickness condition of free stream needs to be considered. Recently some research done on a modified equation of state (Yuan and Schaefer (2006)) to model lower temperature thermodynamic equilibrium was reported.

For low and intermediately high Reynolds number (Roychowdhury and Sreedhar (2000)) for synthetic mixing layer profile analysis was done earlier and convectively unstable system was found for such cases together with absolute instability where viscous dissipation was accounted in small scales. The very large Reynolds number flows (Roychowdhury and Sreedhar (1997)) (inviscid case) showed convectively unstable flows. In the present analysis of high Reynolds number flows, in addition to the seen lower thermo-dynamical non-equilibrium, we also see a complex effect of absolute instability (Roychowdhury et al (2003)) (mixing noise component of jet noise propagating upstream with isotropic dissipation) coexisting with convective (broad band component of jet noise) occurring at high dynamic pressure regions. This interaction between absolute and convective instabilities (Roychowdhury (2005)) is primarily due to shear layer shock interaction in the jet plume and there is a complex interaction of these two types of instabilities in the jet plume where even frequency shifted effects come to existence and complicates the flow field scenario. Turbulence models for high Reynolds number flows should be developed which have to model simultaneously two important flow fields, namely through phenomenological compressibility correction for shear layer effects modeled for accounting convective instabilities and those arising from shock interaction (or absolute instabilities) which need vorticity effects to be modeled. Further isentropic analysis (Roychowdhury et al (2003)) and non-isentropic analysis^{12,13,15,16} (Roychowdhury and Sreedhar (1997), Roychowdhury and Sreedhar (2000), Roychowdhury (2005) and (Roychowdhury et al (2003))) model respectively convective and absolute instability with closed flow analysis (incorporating viscous dissipation).

In addition to turbulence model limitations in the present work, errors due to non-conforming grids used by us in N-S code could contaminate the solution and nullity condition of free stream and frequency shifted effects may become elusive.

5 Conclusions

Here in both the cases we see that frequency shifted phenomena which in this case leads to nullity free stream conditions giving results which sometimes match with experimental data and not sometimes. However as in the previous two cases we think that restriction of occurrence in cold flows need not happen always and may exist in hot co-streams as in combustion chambers. Also some recommend the use of RANS model with compressibility corrections for obtaining base flow results which needs to be tried out.

Acknowledgement

We would like to thank Shri N Janardhan of PARK Engg college, Coimbatore whose MTech thesis was done with me and from which this work grew up.

6 References

- [1] Chapman D. R. (1951) An analysis of base pressure at supersonic velocities and comparison with experiment NACA Rept No 1051.
- [2] Crocco L. and Lees L. (1952) A mixing theory for interaction between dissipative flow and nearly isentropic stream" *Jou of Aeronau Science*, **19**, pp 649- 676.
- [3] Fays J. A. and Riddell F. R. (1958): Theory of stagnation point heat transfer in dissociated air, *Jou of Aeronau Sci.*, **25**, pp 73-85.
- [4] Korst H. H. (1956) A theory for base pressure in transonic and supersonic flow, *Jou of Appl Mech* **23**, pp 593-600.
- [5] Gaster M. (1962) A note on the relation between temporally increasing disturbances in hydrodynamic stability, *J Fluid Mech.*, **14** pp222-24.
- [6] B. H. Goethert B. H. (1961) Base flow characteristics of Missiles with cluster rocket exhausts, American Rocket Society Missile and Space Vehicle Testing Conference, March 13-16..
- [7] Latvala E .R. (1959) Spreading of Rocket exhaust jets at high altitudes, AEDC-TR-59-11, Arnold Eng Develop Cen, Tullahoma.
- [8] Roychowdhury A. P. and Sreedhar, B. N., (1992) Gaster's transform, *AIAA Jou*, **30**, pp2776-78.
- [9] Roychowdhury A.P (1994). Linear stability analysis of compressible mixing layers *PhD thesis, I.I.T Kharagpur, India.*
- [10] Roychowdhury A. P. and Sreedhar B. N., (1997) Non-isentropic, linear stability analysis of compressible mixing layers, *Zeit Appl Math Phys*, **48** (1997) pp774-87.
- [11] Roychowdhury A. P. and Sreedhar B. N. (2000), Viscous non-isentropic, linear stability analysis of compressible mixing layers", *Indian J Engg & Mat. Sci*, **7** pp 8-15.
- [12] Roychowdhury A. P., Kumar P. and Balu R (2000), Prediction of jet-mixing noise of supersonic jets issuing from axisymmetric nozzles, *J Aeronaut Soc India*, **52** pp 216-21.
- [13] Roychowdhury A. P. (2003) Kinematic representation of dynamic Navier Stokes equation", *Acta Ciencia Indica Phy*, **95** pp 283-90.
- [14] Roychowdhury A. P., Kumar P and Balu R, (2003) A critical review of turbulence modeling, *Indian J Radio & Space Phys*, **32**, pp349-59.
- [15] Roychowdhury A. P (2005), Absolute and convective study of weakly compressible mixing layers, *Indian J Radio & Space Phys*, **34** pp106-113.
- [16] Thomas P.D. and Lombart C.K. (1979) Geometric conservative law and its applications in moving grids, *AIAA Jou*, **17** pp1030-39.
- [17] Visbal M.R. and Gaitonde D.V. (2002) On the use of finite difference schemes on curvilinear & deforming grids", *J Compt Phys.*, **181** pp155-85.
- [18] Yuan P & Schaefer L (2006) Equation of state in a lattice Boltzman model, *Phys. Fluids*. **18**, 042101 (pp1-11).